

# Action Potential of Lateral Geniculate Neurons at Low Threshold Currents: Simulation Study

Faris Tarlochan, Siva Mahesh Tangutooru

**Abstract**—Lateral Geniculate Nucleus (LGN) is the relay center in the visual pathway as it receives most of the input information from retinal ganglion cells (RGC) and sends to visual cortex. Low threshold calcium currents (IT) at the membrane are the unique indicator to characterize this firing functionality of the LGN neurons gained by the RGC input. According to the LGN functional requirements such as functional mapping of RGC to LGN, the morphologies of the LGN neurons were developed. During the neurological disorders like glaucoma, the mapping between RGC and LGN is disconnected and hence stimulating LGN electrically using deep brain electrodes can restore the functionalities of LGN. A computational model was developed for simulating the LGN neurons with three predominant morphologies each representing different functional mapping of RGC to LGN. The firings of action potentials at LGN neuron due to IT were characterized by varying the stimulation parameters, morphological parameters and orientation. A wide range of stimulation parameters (stimulus amplitude, duration and frequency) represents the various strengths of the electrical stimulation with different morphological parameters (soma size, dendrites size and structure). The orientation (0-1800) of LGN neuron with respect to the stimulating electrode represents the angle at which the extracellular deep brain stimulation towards LGN neuron is performed. A reduced dendrite structure was used in the model using Bush-Sejnowski algorithm to decrease the computational time while conserving its input resistance and total surface area. The major finding is that an input potential of 0.4 V is required to produce the action potential in the LGN neuron which is placed at 100  $\mu\text{m}$  distance from the electrode. From this study, it can be concluded that the neuroprostheses under design would need to consider the capability of inducing at least 0.4V to produce action potentials in LGN.

**Keywords**—Lateral geniculate nucleus, visual cortex, finite element, glaucoma, neuroprostheses.

## I. INTRODUCTION

**G**LAUCOMA is the major ophthalmological challenge for the eastern Arabian population. Glaucoma destroys retinal ganglion cells (RGC), the neurons which connect the eye to the visual brain. Without these cells, visual signals cannot reach those parts of the central nervous system that give rise to perceptions. Since human ganglion cells do not grown anew and once lost are gone forever, the only practical means of restoring vision to those blinded through glaucoma is a neuroprostheses that interfaces visual neurons of the brain to stimulating electrodes driven by an image capture system and electronic circuitry. This involves navigating the electrodes

and penetrating the brain tissue to reach the target side. One of the identify target side is the lateral geniculate nucleus (LGN) neurons.

LGN neurons have relay neurons that are present along the visual pathway. LGN structure is organized into six layers of which the top four are parvocellular and the bottom two are magnocellular layers [1]. Functionally, these magnocellular layers are known to receive strong drive from parasol RGCs while the parvocellular layers receive strong drive from midget RGCs. These distinct cell functional classes may be identifiable on the basis of their morphological properties [2]-[4]. Morphologically, the neurons in the respective layers also vary in their soma size, number of dendrites, dendritic arborisation, and dendrites orientation. Although there are differing interpretations of the ways in which the morphological and functional variables may be related [5]-[7], an analysis of geniculate organization has been significantly performed to the recognition correlation between functional and morphological variables. Stimulation of LGN neurons of different morphologies produces different firing patterns. These firing patterns are the expressions of the functional mechanism of those neurons. This can significantly be applied for the LGN neuro prosthesis study when neurons lack the input from RGC's due to the neurological disorders like glaucoma. The objective of this study is to investigate the required input potential to produce an action potential in the LGN neuron by means of simulation.

## II. FINITE ELEMENT MODEL

An electrophysiological model of LGN neuron has been developed by using the finite element method in the COMSOL Multiphysics modeling environment. The LGN neuron was modeled as a single compartment with soma and dendrites. A platinum electrode ( $\sigma = 94.35 \times 10^{-5}$  S/m and  $\epsilon_r = 1$ ) of 50  $\mu\text{m}$  diameter with silica insulation ( $\sigma = 10^{-14}$  S/m and  $\epsilon_r = 4.2$ ) was also modeled to provide necessary current stimulus needed for the neuron excitation, with  $\sigma$  and  $\epsilon_r$  being the conductivity and relative permittivity of the material respectively [8]-[10]. LGN neuron and electrode models were coupled by positioning in a homogeneous isotropic volume conductor mimicking the tissue medium as physiological saline ( $\sigma = 1$  S/m and  $\epsilon_r = 80$ ). The tissue domain surrounding the electrode was modeled cylindrically (1.6 mm diameter and 1.6 mm height) with the outer boundary set to 0 V, and the electrode contact set to the stimulus voltage.

The current balanced (1) by a Hodgkin-Huxley type of model was used to model the neuron's plasma membrane. This equation is balanced by the stimulus current and the

Faris Tarlochan is with Qatar University, Doha, Qatar (phone: +974 4403 4367; e-mail: faris.tarlochan@qu.edu.qa).

Siva Mahesh is with Qatar University, Doha, Qatar (Corresponding author, e-mail: sivamahesh@qu.edu.qa).

currents associated with the channels in the cell membrane [11], [12].

$$C \frac{dv}{dt} = I_{sti} - I_T - I_H - I_{Na} - I_{Kdr} - I_{Ks} \quad (1)$$

where  $V$  is the membrane potential,  $C$  ( $= 1 \mu\text{F}/\text{cm}^2$ ) is the membrane capacitance,  $I_{sti}$  is the stimulated current,  $I_T$  is the t-type calcium current,  $I_H$  is the hyperpolarization current,  $I_{Na}$  is the sodium current,  $I_{Kdr}$  is the delayed rectifier potassium current, and  $I_{Ks}$  is slow potassium current. Equation (2) is used to solve for  $I_T$ :

$$I_T = P m_T h_T Z^2 F^2 V \frac{\left( CaI - CaOe^{-\frac{ZFV}{RT}} \right)}{RT \left( 1 - e^{-\frac{ZFV}{RT}} \right)} \quad (2)$$

where  $P$  ( $= 0.0001 \text{ S cm}^{-2}$ ) is the maximum permeability,  $m_T$  and  $h_T$  are the activation and inactivation variables,  $CaO$  ( $= 2 \text{ mV}$ ) and  $CaI$  ( $= 0.00005 \text{ mV}$ ) are the extracellular and the intracellular concentrations of  $\text{Ca}^{2+}$  respectively, and  $Z$  ( $= 2$ ),  $F$  ( $= 96485 \text{ C mol}^{-1}$ ),  $R$  ( $= 8.3144621 \text{ J K}^{-1} \text{ mol}^{-1}$ ), and  $T$  ( $= 309 \text{ K}$ ) are the valence, the Faraday constant, the gas constant and the absolute temperature respectively.

The equations used to solve for  $I_H$ ,  $I_{Na}$ ,  $I_{Kdr}$ , and  $I_{Ks}$  are:

$$I_H = g_h (m_h)^3 (V + 43) \quad (3)$$

$$I_{Na} = g_{Na} (m_{Na})^3 h_{Na} (V - E_{Na}) \quad (4)$$

$$I_{Kdr} = g_{Kdr} (m_{Kdr})^4 (V - E_K) \quad (5)$$

$$I_{Ks} = g_{Ks} (m_{Ks})^3 h_{Ks} (V - E_K) \quad (6)$$

where  $g_h$ ,  $g_{Na}$ ,  $g_{Kdr}$ ,  $g_{Ks}$  are the maximum conductance for their respective channel. While the activation and inactivation variables  $m_T$ ,  $h_T$ ,  $m_h$ ,  $m_{Na}$ ,  $h_{Na}$ ,  $m_{Kdr}$ ,  $m_{Ks}$ , and  $h_{Ks}$  were solved using common solver (7) of variable  $\omega$  with numerical parameters obtained from [11], [12].

$$\frac{d\omega}{dt} = \alpha_\omega (1 - \omega) - \beta_\omega \omega = (\omega_\infty - \omega) / \tau_\omega \quad (7)$$

The model parameters are summarized in the Table I.

In the reduced morphology model with two compartments (one for soma and the other for dendrites), the dendrites are replaced with cylindrical structure conserving the input resistance and the total surface area. The soma sizes simulated are 10, 15, and 20  $\mu\text{m}$  in diameter that represent various sizes in different layers of LGN structure. The dendritic cylinder size parameters are shown in Table II.

TABLE I  
 ELECTRICAL PARAMETERS OF SOMA AND DENDRITES OF NEURON

Variable	Value / Expression
$g_h$	0.0005 S/cm <sup>2</sup>
$g_{Na}$	0.03 S/cm <sup>2</sup>
$g_{Kdr}$	0.003 S/cm <sup>2</sup>
$g_{Ks}$	0.0007 S/cm <sup>2</sup>
$m_{T\infty}$	$\frac{1}{1 + e^{(0.1613(-84 - V))}}$
$\tau_{m_T}$	$0.204 + \frac{0.333}{e^{(0.0599(-135 - V))} + e^{(0.0549(19.8 + V))}}$
$h_{T\infty}$	$\frac{1}{1 + 0.25 e^{(84 + V)}}$
$m_{h\infty}$	$\frac{1}{1 + e^{0.181(85 + V)}}$

The reduced method consists of merging dendritic branches into equivalent cylinder, which preserve the axial resistance of the original branches. If the cross-sectional area of the equivalent cylinder equals the sum of each individual cross-sectional area, this is equivalent to summing parallel resistances because:

$$\frac{1}{r} = \sum_j \left( \frac{1}{R_j} \right) \quad (8)$$

where  $R$  ( $j$ ) are the axial resistances of the collapsed branches.

TABLE II  
 THE MORPHOLOGICAL PARAMETERS OF THE REDUCED DENDRITE STRUCTURE BASED ON THE BUSH-SEJNOWSKI ALGORITHM

Length ( $\mu\text{m}$ )	Diameter ( $\mu\text{m}$ )	Surface Area ( $\mu\text{m}^2$ )	No. of primary dendrites collapsed
70.2	12.3	5425	43508
85.7	8.5	2261	18133
90	7	1979	15871

The radius ( $r$ ) of the equivalent cylinder is then given by:

$$r = \sqrt{\left( \sum_i r_i^2 \right)} \quad (9)$$

where  $r_i$  are the radii of the collapsed branches. The length ( $l$ ) of the equivalent cylinder is taken as an average of the lengths of the collapsed branches ( $l_i$ ), weighted by their respective diameters ( $r_i$ ), such as:

$$l = \frac{\left( \sum_i l_i r_i \right)}{\left( \sum_i r_i \right)} \quad (10)$$

This modification of the Bush-Sejnowski algorithm was added to accommodate the merging of branches of very different length, which is often encountered while reducing dendritic morphologies [13].

Because the total membrane area is not conserved in this method, the reduced model may not have a correct input resistance although the axial resistance is conserved. This is compensated by introducing in each equivalent cylinder a dendritic correction factor ( $C_d$ ), which rescales the values of conductance ( $g_i$ ) and membrane capacitance ( $C_m$ ).  $C_d$  was estimated such that the reduced model has the correct input resistance and time constant. The dendritic correction factor is calculated from the ratio of the total surface area of the dendritic segments to their equivalent cylinders

Stimulation parameters such as amplitude and pulse duration were altered while keeping the frequency constant to 150 Hz as this parameter is believed to be the safe frequency for deep brain stimulation. To alter the morphological parameters such as dendritic population and its size, and soma size, a reduced structure was modeled while conserving the input resistance and total surface area. The orientation of the LGN neuron with respect to stimulating electrode was altered in the range of  $0-180^\circ$ .

### III. RESULTS

The response of the LGN neuron is dependent on the stimulation parameters such as pulse amplitude, pulse duration and frequency. A single pulse was first used to stimulate the LGN neuron with the pulse amplitude ranging 0.1-2 V and the pulse duration 5 ms. The resting membrane potential (RMP) of LGN neuron was maintained at -65 mV.

Fig. 1 shows the firing of the LGN neuron for various input stimulus varying the pulse amplitude. The stimulation is provided by the electrode placed in extracellular medium at 100  $\mu\text{m}$  distance from the neuron. The potential was measured at the surface of the somato dendritic membrane. The channels incorporated are  $I_T$ ,  $I_{Na}$ ,  $I_{Kdr}$ , and  $I_{Ks}$ . The result explains that the input voltage over 0.4 V is required to produce the  $\text{Ca}^{2+}$  spike. The spike initiated immediately after the stimulation by slightly hyperpolarizing and then sharply depolarizing.

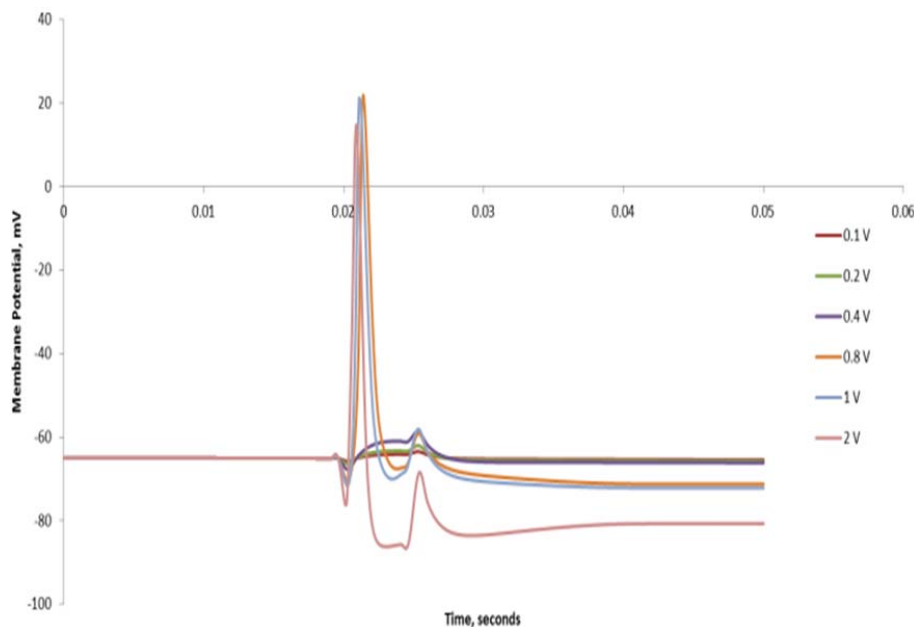


Fig. 1 Generation of  $\text{Ca}^{2+}$  spike when stimulated with varying pulse amplitude and constant 5 ms pulse duration

Keeping the pulse amplitude constant to 1 V and varying the pulse duration from 5 ms to 20 ms, the  $\text{Ca}^{2+}$  spikes generated are shown in Fig. 2. An extended pulse duration did not generate an extra  $\text{Ca}^{2+}$  spikes but maintained a constant membrane potential above the RMP at -59 mV after the  $\text{Ca}^{2+}$  spike. Instead of applying constant 1 V for long duration, a short duration stimulus of 5 ms at 150 hz frequency was applied. Then a continuous firing of LGN neuron was observed at the membrane surface as shown in Fig. 3.

This illustrates that the LGN neuronal membrane is in tonic mode where each stimulus spike generates one action potential spike and thereby preventing its membrane potential to hyperpolarize (potentials higher than RMP) which will lead to burst mode.

The contribution of each current during the TC neuron

firing after electrical stimulation was also studied. A 1 V extracellular stimulation for 5 ms from 100  $\mu\text{m}$  distance was applied while currents are measured at the somato dendritic surface.  $I_t$  is the t-type calcium current,  $I_{Na}$  is the sodium current,  $I_k$  is the delayed rectified potassium current,  $I_{ka}$  is the slow potassium current and  $I_c$  is the membrane capacitive current. It can be seen that the somato dendritic membrane current density is the highest with the sodium current.

In the reduced model with only two voltage-dependent currents,  $I_T$ ,  $I_H$ , and leakage currents shows the basic features of generation of  $\text{Ca}^{2+}$  spikes. The baseline membrane potential is now shifted to -70 mV towards the hyperpolarized membrane potential. When the stimulus was applied to the neuron in the hyperpolarized state, the  $\text{Ca}^{2+}$  spikes were generated continuously as shown in Fig. 5.

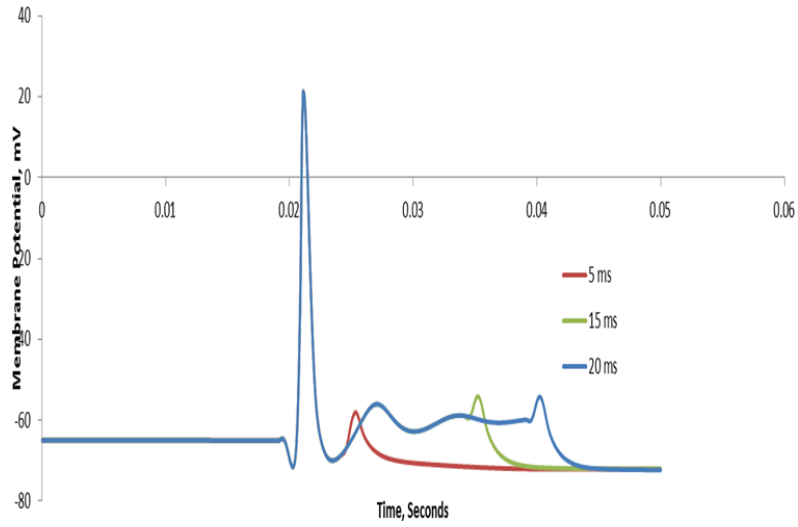


Fig. 2 Generation of  $Ca^{2+}$  spike when stimulated with varying pulse duration and constant 1 V pulse amplitude

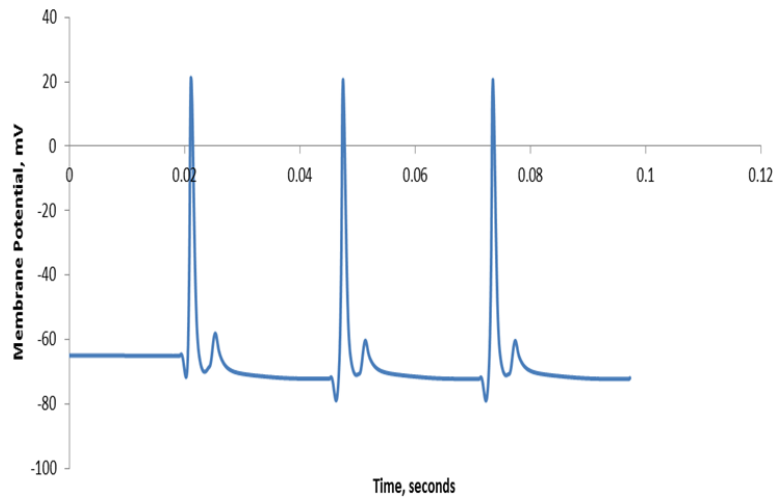


Fig. 3 Continuous firing of LGN neurons when stimulated with stimulus of 5 ms pulse duration, 1 V pulse amplitude and 150 Hz frequency.

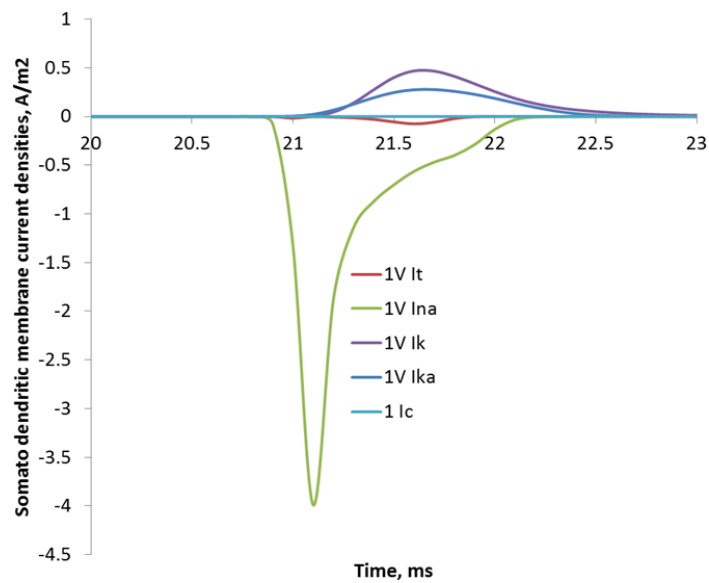


Fig. 4 1V extracellular stimulation

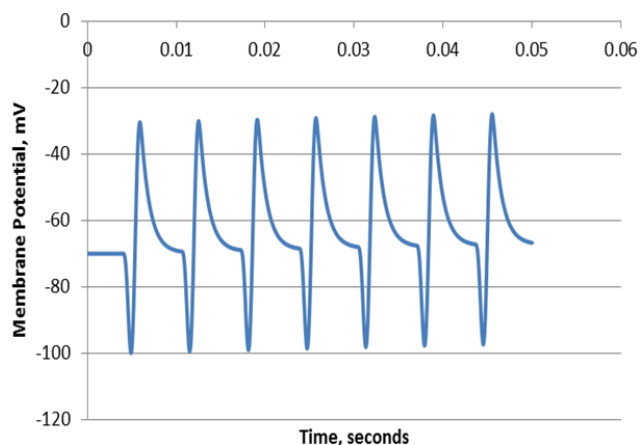


Fig. 5 Continuous firing of LGN neurons when stimulated with stimulus of 0.1 ms pulse duration, 1 V pulse amplitude and 150 Hz frequency

#### IV. CONCLUSION

Glaucoma is the major ophthalmological challenge for the eastern Arabian population. Glaucoma destroys retinal ganglion cells (RGC), the neurons which connect the eye to the visual brain. Since human ganglion cells do not grow anew and once lost are gone forever, the only practical means of restoring vision to those blinded through glaucoma is a neuroprosthesis. One of the identify target side for the neuroprosthesis is the lateral geniculate nucleus (LGN) neurons. This research studied the action potential of LGN based on a range of input potentials. This is an important aspect in the designing of neuroprosthesis. From this study, it was found that an input potential of 0.4 V is required to produce the action potential in the LGN neuron which is placed at 100  $\mu\text{m}$  distance from the electrode. Besides this it was also found that the sodium current has a higher influence on the somato dendritic membrane current than any other currents studied.

#### ACKNOWLEDGMENT

This research was made possible by the NPRP grant #NPRP5-457-2-181 from the Qatar National Research Fund (a member of Qatar Foundation). The statements made herein are solely the responsibility of the authors.

#### REFERENCES

- [1] K. A. Schneider, M. C. Richter, and S. Kastner, "Retinotopic organization and functional subdivisions of the human lateral geniculate nucleus: a high-resolution functional magnetic resonance imaging study.," *J. Neurosci.*, vol. 24, no. 41, pp. 8975–85, Oct. 2004.
- [2] T. L. Hickey and R. W. Guillery, "A study of Golgi preparations from the human lateral geniculate nucleus.," *J. Comp. Neurol.*, vol. 200, no. 4, pp. 545–77, Aug. 1981.
- [3] R. Zomorodi, A. S. Ferecskó, K. Kovács, H. Kröger, and I. Timofeev, "Analysis of morphological features of thalamocortical neurons from the ventroposterolateral nucleus of the cat," *J. Comp. Neurol.*, vol. 518, no. 17, pp. 3541–3556, 2010.
- [4] R. W. Guillery, "A study of Golgi preparations from the dorsal lateral geniculate nucleus of the adult cat.," *J. Comp. Neurol.*, vol. 128, no. 1, pp. 21–50, 1966.

- [5] S. LeVay and D. Ferster, "Relay cell classes in the lateral geniculate nucleus of the cat and the effects of visual deprivation.," *J. Comp. Neurol.*, vol. 172, no. 4, pp. 563–84, Apr. 1977.
- [6] L. Stanford, M. Friedlander, and S. Sherman, "Morphology of physiologically identified W-cells in the C laminae of the cat's lateral geniculate nucleus.," *J. Neurosci.*, vol. 1, no. 6, pp. 578–584, Jun. 1981.
- [7] B. Dreher, Y. Fukada, and R. W. Rodieck, "Identification, classification and anatomical segregation of cells with X-like and Y-like properties in the lateral geniculate nucleus of old-world primates.," *J. Physiol.*, vol. 258, no. 2, pp. 433–452, Jun. 1976.
- [8] V. Crunelli, S. Lightowler, and C. E. Pollard, "A T-type  $\text{Ca}^{2+}$  current underlies low-threshold  $\text{Ca}^{2+}$  potentials in cells of the cat and rat lateral geniculate nucleus.," *J. Physiol.*, vol. 413, no. 1, pp. 543–561, Jun. 1989.
- [9] H. Jahnsen and R. Llinás, "Electrophysiological properties of guinea-pig thalamic neurones: an in vitro study.," *J. Physiol.*, vol. 349, pp. 205–26, Apr. 1984.
- [10] H. Jahnsen and R. Llinás, "Ionic basis for the electro-responsiveness and oscillatory properties of guinea-pig thalamic neurones in vitro.," *J. Physiol.*, vol. 349, no. 1, pp. 227–247, Apr. 1984.
- [11] Y. Amarillo, G. Mato, and M. S. Nadal, "Analysis of the role of the low threshold currents  $I_T$  and  $I_h$  in intrinsic delta oscillations of thalamocortical neurons," *Front. Comput. Neurosci.*, vol. 9, no. May, pp. 1–9, 2015.
- [12] C. C. McIntyre, W. M. Grill, D. L. Sherman, and N. V. Thakor, "Cellular effects of deep brain stimulation: model-based analysis of activation and inhibition.," *J. Neurophysiol.*, vol. 91, no. 4, pp. 1457–1469, 2004.
- [13] Destexhe, M. Neubig, D. Ulrich, and J. Huguenard, "Dendritic low-threshold calcium currents in thalamic relay cells.," *J. Neurosci.*, vol. 18, no. 10, pp. 3574–3588, 1998.

**Faris Tarlochan** is a Professor and Program Coordinator of the Mechanical Engineering Program at Qatar University. He obtained his BSc in Mechanical Engineering and MSc in Biomedical Engineering from Purdue University, USA. His PhD is from University Putra Malaysia. He is a Chartered Engineering with the Engineering Council of UK and a Fellow with the Institution of Mechanical Engineers UK. His research interest includes prostheses design, applied mechanics and computational mechanics.

**Siva Mahesh Tangutooru** received the B.E. degree from Osmania University, India and M.S. & Ph.D. degrees from Louisiana Tech University, USA. All the degrees received are in biomedical engineering. He is currently working as a post-doctoral researcher at Qatar University, Qatar. His research interests are Lab-on-a-chip applications and neural engineering.